JACS
JOURNAL OF THE AMERICAN CHEMICAL SOCIETY
Communication
pubs.acs.org/JACS

Electrodeposition of a Pt Monolayer Film: Using Kinetic Limitations for Atomic Layer Epitaxy

Sylvain Brimaud and R. Jürgen Behm*

Institute of Surface Chemistry and Catalysis, Ulm University, Albert-Einstein-Allee 47, D-89063 Ulm, Germany

Supporting Information

ABSTRACT: A new and facile one-step method to prepare a smooth Pt monolayer film on a metallic substrate in the absence of underpotential deposition-type stabilizations is presented as a general approach and applied to the growth of Pt monolayer films on Au. The strongly modified electronic properties of these films were demonstrated by in situ IR spectroscopy at the electrified solid−liquid interface with adsorbed carbon monoxide serving as a probe molecule. The Pt monolayer on Au is kinetically stabilized by adsorbed CO, inhibiting further Pt deposition in higher layers.

Monolayer films deposited on a heterometal substrate and the resulting modified metal surfaces have received considerable attention during recent years because of their interesting and often very promising (electro-)chemical and (electro-)catalytic properties, which often deviate drastically from those of the respective bulk materials.[1−3] This has been utilized to design tailor-made bimetallic structures as optimized catalysts for electrocatalytic reactions such as the O_2 reduction reaction[4,5] and electro-oxidation of small oxygenated aliphatic compounds.[6] For a detailed, quantitative understanding of the underlying physical effects and for comparison with theory, extended single-crystal electrodes covered by monolayer metal films have frequently been used as model systems.[3,7,8] Traditionally, monolayer metal films have been produced at electrified solid−liquid interfaces by underpotential deposition (upd), that is, deposition at potentials higher than the redox potential required for metallic reduction (the Nernst potential), exploiting the fact that the substrate−deposit interactions are stronger than the deposit−deposit interactions.[9] However, in many cases (e.g., the reduction of platinate ions on gold surfaces), the energetics do not allow for this approach, and the onset potential of deposition coincides with that for bulk deposition,[10,11] leading to rough films with three-dimensional (3D) structures.[11] To circumvent this problem, other methods have been designed to (apparently) produce smooth monolayer films. For instance, Brankovic et al.[12] proposed an elegant procedure involving the use of a predeposited sacrificial copper monolayer where monatomic-height Pt clusters (submonolayer coverage) are formed after galvanic replacement. Later, this method was extended, and the preparation of Pt monolayer (Pt-ML)-modified electrodes and electrocatalysts has been claimed.[5,6,13] However, as will become obvious in the following, the resulting Pt films are far from perfect monolayer films.

Here we describe a method that allows smooth and essentially perfect Pt-ML films to be grown in the absence of upd-type energetic stabilizations. It is based on kinetic effects that hinder the continuing metal deposition after completion of the first monolayer, which resembles the situation in atomic layer epitaxy.[14,15] This method is of general applicability for a variety of different metal-on-metal systems. Specifically, we were able to prepare a smooth Pt-ML film on polycrystalline gold using kinetic limitations, overcoming the energetic limitations (absence of Pt upd) mentioned above, as demonstrated by in situ IR spectroelectrochemistry and coulometric analysis. Atypical IR vibrational properties of adsorbed CO (CO_{ad}) were identified and attributed to surface strain and substrate (electronic) effects, in agreement with modern surface science concepts. To the best of our knowledge, these are the first IR spectroscopic data available for the Au/Pt-ML/CO_{ad} system.

Details on the experimental setup for in situ IR spectroscopy in an attenuated total reflection (ATR) configuration under well-defined mass transport conditions are given elsewhere,[16] as is the procedure for preparing polycrystalline Au films on Si prisms by electroless deposition[17,18] [also see the Supporting Information (SI)]. A 0.1 mM solution of K_2PtCl_4 in 0.5 M H_2SO_4 was protected from light, CO-saturated, and then introduced into the thin-layer flow cell by electrolyte exchange of the initial CO-free 0.5 M H_2SO_4 supporting electrolyte. This operation was performed under potential control at E = 0.30 V vs RHE. One should note that this potential is far below the Nernst redox potential of the Pt^{2+}/Pt couple (0.76 V vs RHE). Thus, continuing Pt bulk deposition would be expected. However, as shown in Figure 1a, this was obviously not the case, and a distinct reduction peak was recorded. The process was very fast (ca. 50 s) and highly reproducible. The current peak is attributed to the reduction of Pt ions to Pt metal on the Au surface and demonstrates that deposition ceased (i.e., the current decayed to 0) as soon as a saturation Pt coverage was reached. We propose that immediately after Pt deposition of the first layer, this layer is covered by adsorbed CO and thus poisoned for further Pt deposition, as the CO_{ad}-blocked Pt sites inhibit further reduction of the continuously supplied Pt ions, preventing bulk Pt formation.

Simultaneously recorded in situ IR spectra (Figure 1b) showed two bands at 2061 and 1890 cm^{-1} that are attributed to linearly and bridge-bonded Pt−CO_{ad}, respectively (see below). A weak band at 2119 cm^{-1} (labeled with stars in Figure 1b)

Received: May 23, 2013
Published: August 2, 2013

dx.doi.org/10.1021/ja4051795 | J. Am. Chem. Soc. 2013, 135, 11716−11719

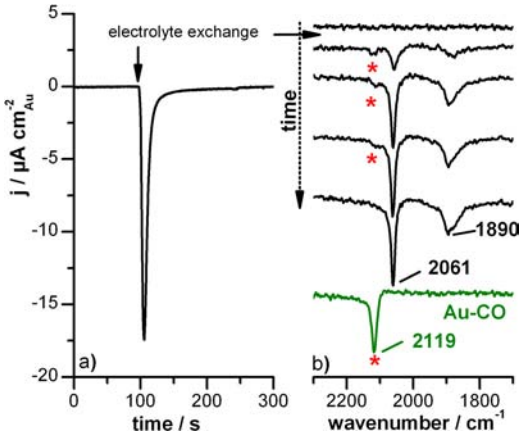

Figure 1. (a) Current transient at constant potential upon electrolyte exchange from the supporting electrolyte to a CO-saturated electrolyte containing 0.1 mM K_2PtCl_4 (0.5 M H_2SO_4, E = 0.30 V vs RHE). (b) Simultaneously acquired ATR-IR spectra (detail of the CO_{ad} vibrational region only). The spectrum of adsorbed CO on a polycrystalline Au film (green line) is also shown for comparison.

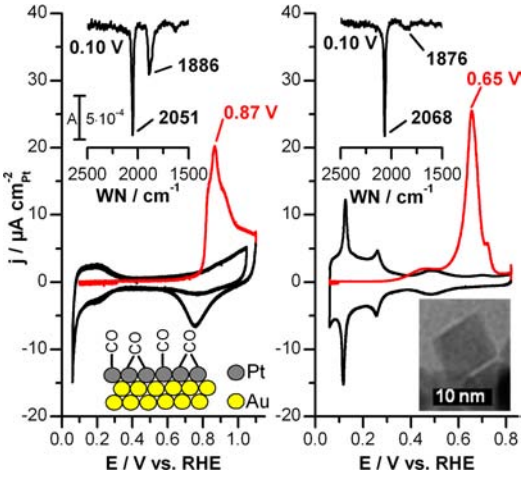

Figure 2. Red traces: potentiodynamic removal of a saturated CO adlayer (CO_{ad} stripping voltammograms, 5 mV s^{-1}) in CO-free 0.5 M H_2SO_4 electrolyte on the Pt-ML electrode (left panel) and on 10 nm Pt(111) octahedrons (right panel). Black traces: base cyclic voltammograms. Bottom insets: schematic representation of the Pt-ML (left) and a bright-field transmission electron microscopy image of a nanooctahedron (right). Top insets: ATR-IR spectra of the respective electrodes at E = 0.10 V vs RHE in the absence of dissolved CO (CO_{ad} vibrational region only).

disappeared with increasing Pt coverage. The latter feature is associated with CO_{ad} on the Au surface, which exists in a dynamic equilibrium with CO dissolved in the electrolyte, as evidenced by an IR spectrum recorded in the absence of dissolved Pt(II) salt (green trace in Figure 1b). Both the electrochemical and spectroscopic data indicated complete coverage of the Au surface by Pt−CO_{ad}. Moreover, the charge under the reduction peak, 195 μC per square centimeter of Au electrochemical surface area (cm^2_{Au}), corresponds to the formation of a complete Pt-ML, assuming (i) a surface density of 1.25×10^{15} atoms/cm^{-2} for polycrystalline Au[19] and (ii) that $PtCl_4^{2-}$ was transformed to the Pt(I) complex $[Pt_2Cl_4(CO)_2]^{2-}$ when CO was bubbled into the acidic solution of the Pt(II) salt.[20] Contributions from other Faradaic processes, in particular from adsorbed anion displacement, were assumed to be negligible. Thus, the method derived here enables the facile preparation of a CO_{ad}-saturated Pt-ML on a Au electrode.

After switching back to 0.5 M H_2SO_4 supporting electrolyte and completely purging the flow cell to remove the dissolved CO and Pt ions, we decreased the electrode potential to 0.10 V vs RHE. In Figure 2 we compare the CO_{ad} vibrational spectrum at 0.10 V vs RHE and the CO_{ad} stripping voltammograms recorded for the as-prepared Pt−CO_{ad} monolayer on the one hand and similar data obtained for a saturated CO adlayer on 10 nm Pt(111) octahedrons supported on a Au film on the other hand (see refs 17 and 21 for details about the preparation of shape-selected nanocrystals). Both the spectroscopic and voltammetric data for the Pt(111) nanooctahedrons exhibit features characteristic of single-crystalline Pt(111) electrodes, indicating well-ordered nanocrystal surfaces (facets), as expected from the crystal shape, and they differ from the data for a classical polycrystalline Pt electrode (qualitative and quantitative analyses of these features are discussed in refs 17, 21, and 22). A considerable red shift (ca. 17 cm^{-1}) for the linearly adsorbed CO (CO_l) band on the Pt-ML deposited on the Au electrode relative to the CO_l band on Pt(111) octahedrons indicates stronger binding of CO_{ad} on the Pt-ML surface, in agreement with expectations based on the d-band model.[2] This is accompanied by a potential shift of the stripping peak for CO_{ad} on the Pt-ML to more positive values by >0.20 V, indicating that the catalytic properties of the Pt-ML film differ significantly from those of bulk Pt. A larger CO_{ad} binding energy on a Pt-ML film evaporated on single-crystalline Au(111) under ultrahigh vacuum conditions relative to the binding energy on bulk Pt(111) was previously detected by temperature-programmed desorption measurements under vacuum conditions and explained by an upshift of the Pt d-band center due to tensile strain in the surface layer.[23] A blue shift (ca. 10 cm^{-1}) for the bridge-bonded CO_{ad} (CO_b) IR band and its relatively large fraction of the overall CO_{ad} clearly illustrate the influence of the underlying Au substrate on the electronic properties of the Pt-ML film. The influence of the substrate is also reflected by the smaller difference between CO_l and CO_b band frequencies ($\Delta\nu$ = 165 cm^{-1} for the Pt-ML sample compared with 192 cm^{-1} for the Pt(111) octahedrons).

The Pt-ML film differed significantly from Pt deposits resulting from galvanic displacement of a Cu-ML, as indicated by comparison of the IR spectra in Figure 2 with the vibrational properties of CO_{ad} on Pt deposits resulting from galvanic displacement of a Cu-ML (Figure 3a; also see the SI). Most obvious is the distinct presence of a Au−CO band at 2109 cm^{-1} for the latter film surfaces, indicative of substantial amounts of Pt-free surface area or Au surface atoms in the these adlayers, while the intensity in the Au−CO band is negligible for the Pt-ML film prepared in this work. In CO-free electrolyte, the irreversibly adsorbed CO on the Pt deposit exhibited IR characteristics typical of CO adsorbed on Pt nanoparticles.[24,25] Subsequent potentiodynamic oxidation of the adsorbed CO also confirmed the IR-based interpretation (see the SI). Furthermore, there were substantial shifts in the CO_l and CO_b band positions, which shall be discussed below (and SI). Overall, the data indicate that the apparent Pt-ML film generated by galvanic displacement of a Cu-ML film is in reality a layer of Pt cluster agglomerates, as illustrated schematically in Figure 3a (right).

To test the stability of the as-prepared Pt-ML, we recorded IR spectra after oxidative stripping of the pristine CO adlayer and readsorption of CO at 0.10 V vs RHE. The resulting

dx.doi.org/10.1021/ja4051795 | J. Am. Chem. Soc. 2013, 135, 11716−11719

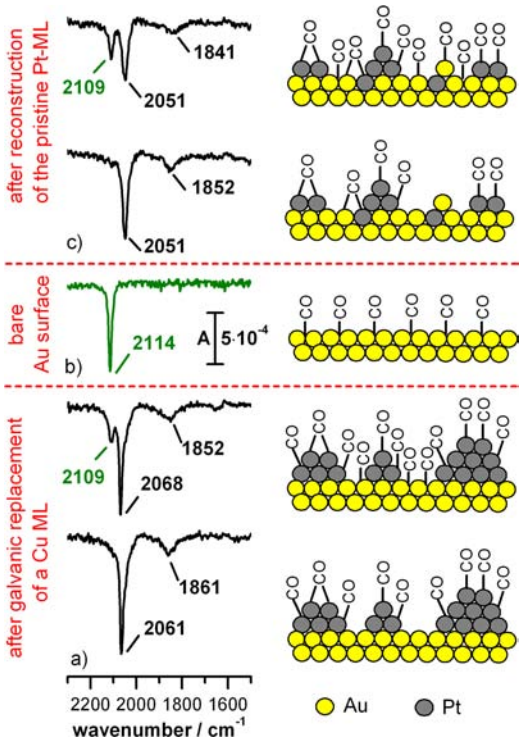

Figure 3. Comparison of the CO_{ad} vibrational ATR-IR spectra (a) for the Pt deposit obtained after galvanic displacement of a Cu-ML in CO-saturated (top) and CO-free (bottom) electrolyte, (b) for the polycrystalline Au film in CO-saturated electrolyte and (c) for the reconstructed Pt-ML in CO-saturated (top) and CO-free (bottom) electrolyte after potentiodynamic oxidative removal of the pristine CO adlayer (E = 0.10 V vs RHE, 0.5 M H_2SO_4). Schematic representations of the corresponding electrode surfaces are provided on the right side of the figure.

spectra (Figure 3c) differ significantly from that of the pristine CO adlayer in Figure 2, indicating a restructuring of the Pt-ML on the Au surface. Hence, either the smooth Pt-ML film is unstable by itself and stabilized only by the presence of the CO adlayer or the potential excursion during CO_{ad} stripping leads to a potential-induced restructuring of the Pt-ML film. The conclusion of irreversible restructuring of the Pt-ML is supported by a clearly visible IR band associated with CO adsorbed on Au surface atoms in CO-containing electrolyte. The oxidative removal of the stabilizing pristine CO adlayer probably results in 3D clustering of the Pt surface atoms because of the energetically more favorable Pt−Pt interactions. After removal of the CO dissolved in the electrolyte, only the IR bands corresponding to strongly adsorbed CO on the restructured Pt-ML are visible (Figure 3c). Their lower intensity in CO-free electrolyte relative to that of the pristine CO saturated Pt-ML (Figure 2) indicates a decrease in the amount of Pt surface atoms, which is consistent with clustering of the Pt-ML when the adsorbed CO is removed by potentiodynamic oxidation. Both the CO_l and CO_b IR bands were red-shifted relative to those for the Pt(111) octahedrons and exhibited a higher (compared with the Pt-ML) $\Delta\nu$ value of 200 cm^{-1}, which is comparable to those for Pt deposits resulting from galvanic displacement of a Cu-ML (Figure 3a) or for porous Pt films.[17] A red shift of both CO_{ad} IR bands is consistent with previous findings of similar shifts with decreasing Pt nanoparticle size,[24,25] which also confirms the interpration of clustering of the initial Pt-ML. Also, the CO_l/CO_b intensity ratio on the restructured Pt-ML seems to be comparable to that on other Pt surfaces, indicating that the substrate influence on the CO_{ad} population probed by IR largely vanished after restructuring, which further supports 3D cluster formation.

In summary, we have developed a new and facile method for the controlled electrochemical growth of structurally well-defined Pt monolayer films on Au electrodes. In situ IR spectroscopy of adsorbed CO revealed distinct electronic ligand and strain effects, indicative of an electronic modification of the Pt monolayer as compared with bulk Pt(111), and confirmed the monolayer geometry, in contrast to the previously reported procedure of preparing so-called Pt monolayer films by galvanic displacement of a sacrificial Cu monolayer, which results in rough agglomerate films rather than in smooth Pt monolayers. Spectroscopic data further revealed that oxidative removal of the CO adlayer results in a distinct restructuring of the Pt films, yielding 3D Pt nanostructures. The method for monolayer film preparation presented here is proposed to be generally applicable for growth systems where monolayer growth is not facilitated by stabilization via underpotential deposition.

■ ASSOCIATED CONTENT

Ⓢ Supporting Information

Experimental details. This material is available free of charge via the Internet at http://pubs.acs.org.

■ AUTHOR INFORMATION

Corresponding Author

juergen.behm@uni-ulm.de

Notes

The authors declare no competing financial interest.

■ ACKNOWLEDGMENTS

This work was supported by the Deutsche Forschungsgemeinschaft (BE 1201/17-1).

■ REFERENCES

(1) Rodriguez, J. A.; Goodman, D. W. *Science* **1992**, *257*, 897.
(2) Hammer, B.; Nørskov, J. K. *Adv. Catal.* **2000**, *45*, 71.
(3) Schlapka, A.; Lischka, M.; Gross, A.; Käsberger, U.; Jakob, P. *Phys. Rev. Lett.* **2003**, *91*, No. 016101.
(4) Zhang, J.; Sasaki, K.; Sutter, E.; Adzic, R. R. *Science* **2007**, *315*, 220.
(5) Adzic, R.; Zhang, J.; Sasaki, K.; Vukmirovic, M.; Shao, M.; Wang, J.; Nilekar, A.; Mavrikakis, M.; Valerio, J.; Uribe, F. *Top. Catal.* **2007**, *46*, 249.
(6) Li, M.; Liu, P.; Adzic, R. R. *J. Phys. Chem. Lett.* **2012**, *3*, 3480.
(7) Kibler, L. A.; El-Aziz, A. M.; Hoyer, R.; Kolb, D. M. *Angew. Chem., Int. Ed.* **2005**, *44*, 2080.
(8) Greeley, J.; Nørskov, J. K.; Kibler, L. A.; El-Aziz, A. M.; Kolb, D. M. *ChemPhysChem* **2006**, *7*, 1032.
(9) Kolb, D. M. *Adv. Electrochem. Electrochem. Eng.* **1978**, *11*, 125.
(10) Uosaki, K.; Ye, S.; Naohara, H.; Oda, Y.; Haba, T.; Kondo, T. *J. Phys. Chem. B* **1997**, *101*, 7566.
(11) Waibel, H. F.; Kleinert, M.; Kibler, L. A.; Kolb, D. M. *Electrochim. Acta* **2002**, *47*, 1461.
(12) Brankovic, S. R.; Wang, J. X.; Adzic, R. R. *Surf. Sci.* **2001**, *474*, L173.
(13) Rincón, A.; Pérez, M. C.; Gutiérrez, C. *Electrochim. Acta* **2010**, *55*, 3152.
(14) Kim, Y. G.; Kim, J. Y.; Vairavapandian, D.; Stickney, J. L. *J. Phys. Chem. B* **2006**, *110*, 17998.
(15) Suntola, T. *Mater. Sci. Rep.* **1989**, *4*, 261.

(16) Chen, Y.-X.; Heinen, M.; Jusys, Z.; Behm, R. J. *Angew. Chem., Int. Ed.* **2006**, *45*, 981.
(17) Brimaud, S.; Jusys, Z.; Behm, R. J. *Electrocatalysis* **2011**, *2*, 69.
(18) Miyake, H.; Ye, S.; Osawa, M. *Electrochem. Commun.* **2002**, *4*, 973.
(19) Trasatti, S.; Petrii, O. A. *Pure Appl. Chem.* **1991**, *63*, 711.
(20) Goggin, P. L.; Goodfellow, R. J. *J. Chem. Soc., Dalton Trans.* **1973**, 2355.
(21) Solla-Gullón, J.; Rodríguez, P.; Herrero, E.; Aldaz, A.; Feliu, J. M. *Phys. Chem. Chem. Phys.* **2008**, *10*, 1359.
(22) Solla-Gullón, J.; Vidal-Iglesias, F. J.; López-Cudero, A.; Garnier, E.; Feliu, J. M.; Aldaz, A. *Phys. Chem. Chem. Phys.* **2008**, *10*, 3689.
(23) Pedersen, M. O.; Ruban, A.; Stensgard, I.; Nørskov, J. K.; Besenbacher, F. *Surf. Sci.* **1999**, *426*, 395.
(24) Park, S.; Wasileski, S. A.; Weaver, M. J. *J. Phys. Chem. B* **2001**, *105*, 9719.
(25) Maillard, F.; Savinova, E. R.; Simonov, P. A.; Zaikovskii, V. I.; Stimming, U. *J. Phys. Chem. B* **2004**, *108*, 17893.